serval
serveur académique lausannois

UNIL | Université de Lausanne
Faculté de biologie et de médecine

Impaired IRE1 expression and XBP1 activation is a hallmark of GCB diffuse large B-cell lymphomas and contributes to tumor growth.

Bojan Bujisic[1], Aude De Gassart[1], Rémy Tallant[1], Olivier Demaria[2], Léa Zaffalon[1], Sonia Chelbi[1], Michel Gilliet[2], Francesco Bertoni[3] and Fabio Martinon[1*]

[1] Dept. of Biochemistry, University of Lausanne, 155 Ch. des Boveresses, Epalinges 1066, Switzerland

[2] Department of Dermatology, CHUV, Lausanne 1011, Switzerland

[3] Lymphoma and Genomics Research Program, IOR Institute of Oncology Research, and IOSI Oncology Institute of Southern Switzerland, Bellinzona, Switzerland

Correspondence to FM:

Fabio.Martinon@unil.ch; Tel.: +41-21-692.5695

Running Title: IRE1 deficiency is a hallmark of GCB DLBL

Keywords: Diffuse Large B cell Lymphoma / ERN1 / ER-stress / unfolded protein response

Number of words for main text: 3891

Key Points:

- GCB DLBCL are characterized by a defective IRE1-XBP1 pathway
- XBP1 expression reduces GCB DLBCL tumour growth in a mouse xenograft model

Abstract:

The endoplasmic reticulum kinase IRE1 and its downstream target XBP1 drive B cell differentiation towards plasma cells and have been shown to contribute to multiple myeloma development; yet little is known on the role of this pathway in Diffuse Large B cell Lymphoma (DLBCL). Here we show that in Germinal Center B cell-like (GCB) DLBCL subtype, IRE1 expression is reduced to a level that prevents XBP1 activation. Gene expression profiles indicated that, in GCB DLBCL cancer samples, expression of *IRE1* mRNA was inversely correlated with the levels and activity of the epigenetic repressor, histone methyltransferase EZH2. Correspondingly, in GCB derived cell lines, the *IRE1* promoter carried increased levels of the repressive epigenetic mark H3K27me3. Pharmacological inhibition of EZH2 erased those marks and restored IRE1 expression and function in vitro and in vivo. Moreover, reconstitution of the IRE1 signaling pathway, by expression of the XBP1 active form, compromised GCB DLBCL tumor growth in a mouse xenograft cancer model. These findings indicate that IRE1-XBP1 downregulation distinguishes GCB DLBCL from other DLBCL subtypes and contributes to tumor growth.

Introduction

Diffuse Large B cell Lymphoma (DLBCL) represents the most common category of Non-Hodgkin Lymphomas and accounts for 30 to 40% of the newly diagnosed patients [1]. Gene expression profiling of patient-derived DLBCL tumors has uncovered two main and noticeably distinct DLBCL molecular subtypes [2,3]. Activated B cell-like or ABC DLBCL subtype is characterized by expression of genes typically induced during *in vitro* activation of peripheral B cells. Most prominent oncogenic events that characterize ABC lymphomas include constitutive NFκB signaling [4-9] and frequent genetic inactivation of Blimp1, a master regulator of terminal plasma B cell differentiation [10,11].

The second main molecular subtype exhibits transcriptional programs characteristic of germinal center B cells and is named Germinal Center B cell-like or GCB DLBCL. This subtype is characterized by overexpression of BCL6 [12], a transcriptional suppressor that down-regulates genes involved in plasma cell differentiation [13,14] and contributes to disease onset by blocking B cells in the germinal center stage [15,16]. Histone methyl-transferase EZH2 is another frequently mutated [17,18] transcriptional regulator that co-operates with aberrant BCL6 activity to promote GCB DLBCL pathology [19,20]. EZH2, the catalytic subunit of the Polycomb Repressor Complex 2, mediates Histone 3 Lysine 27 methylation (H3K27me3) leading to chromatin condensation and repression of its target genes [21,22]. Similar to BCL6, mutated EZH2 permanently down-regulates genes involved in plasma cell differentiation, including Blimp1 and IRF4 [23], and thereby blocks terminal differentiation to promote disease development. Therefore, constitutive inhibition of differentiation programs represents a general strategy that GCB DLBCL deploy to promote tumor growth.

B cell differentiation towards plasma cells is also highly dependent on functional IRE1 signaling [24-26]. IRE1 is a ubiquitously expressed transmembrane kinase and endoribonuclease localized within the Endoplasmic Reticulum (ER). IRE1 detects stress caused by misfolded proteins that accumulate within the ER lumen. Upon activation, IRE1 mediates XBP1 mRNA maturation leading to production of the transcription factor XBP1s that translocates to the nucleus to trigger the expression of ER stress response genes such as *DNAJB9*, *SEC23b* and *SRPR*. In addition to its main role in catalyzing XBP1 mRNA maturation, IRE1 can degrade several mRNA molecules in a process called Regulated IRE1-dependent decay (RIDD) [27]. Upon exposure to stress the signaling pathways steaming from IRE1 promote increased ER folding capacity and restore homeostasis [28,29]

In plasma cells, the IRE1-XBP1s signaling expands the ER network in order to equip these secretory cells with extensive ER folding machinery competent of handling large amounts of immunoglobulins [30]. In addition, XBP1s binds the IL6 promoter, leading to production of this cytokine that is required for appropriate plasma cell differentiation [24]. Intriguingly, constitutive expression of the IRE1-downstream product XBP1s in murine B cells promotes a disease that resembles multiple myeloma (MM) [31]. Furthermore, pharmacological inhibition of the IRE1 activity has been described as a promising therapeutic option in MM indicating addiction of plasma cell derived cancers to IRE1-XBP1s signaling pathway [32,33].

While the importance of the IRE1-XBP1 pathway in multiple myeloma is well established, the role of this pathway in Diffuse Large B Cell Lymphoma remains rather unclear. Comparison between molecular characteristics of ABC and GCB DLBCL subtypes indicated a dichotomy in expression of XBP1s target genes [34]. However, the causes and therapeutic significance of this dichotomy was unknown. Here we describe that specific downregulation of IRE1 expression

impairs XBP1s production and renders GCB DLBCL more sensitive to ER stress inducing agents. The analysis of *IRE1* expression, in a cohort of 350 DLBCL patients, confirmed that IRE1 is specifically downregulated in GCB DLBCL, therefore suggesting that IRE1 levels could serve as a novel marker in DLBCL classification. We identified the epigenetic regulator EZH2 as a key factor that predefined basal levels of IRE1 expression. Pharmacological inhibition of EZH2 enzymatic activity restored IRE1 expression and function in GCB DLBCL. Moreover, reconstitution of the IRE1 pathway by ectopic XBP1s expression compromised tumor growth in a GCB DLBCL xenograft mouse model. This indicates that, in contrast to its tumor-promoting role in multiple myeloma, the IRE1-XBP1s activity might negatively impact tumor growth in GCB DLBCL.

Materials and Methods

Methods for ***Cell culture and Drug Treatment, Immunoblot analysis, Chromatin immunoprecipitation (ChIP), RT-PCR, XBP1 splicing assay and Lentivirus production and cell lines infection*** are detailed described in the Supplemental section.

Mice

Animal experiments were approved by the Veterinary Office of the Canton de Vaud and the Animal Ethics Committee (authorization 2883). Immuno-compromised AGR 129 (IFN-α/β, IFN-γ receptor and RAG-2 deficient) mice were provided by M. Gilliet (Department of dermatology, CHUV, Lausanne) and housed at the University of Lausanne in accordance to local and national guidelines. Six to eight-week-old females were randomly distributed in two groups

and tumor cells were injected subcutaneously in 200μl volume of 1:1 PBS:Matrigel (BD Biosciences). Each mouse was injected with 3 x 10^6 SUDHL4 cells in the left flank and the same number of SUDHL4-XBP1s cells (SUDHL4 infected with the vector expressing XBP1s under Doxycycline) was injected in the right flank. The same experimental procedure was followed to generate the ABC xenograft mouse model using 2.5 x 10^6 HBL1 or HBL1-XBP1s cells (HBL1 infected with the vector expressing XBP1s under Doxycycline). Control group was treated with vehicle (5% sucrose in H_2O). Second group was treated with Doxycycline (5% sucrose, 1 mg/ml Doxycycline in H_2O). Treatments were administered orally through water. Bottles with vehicle or Doxycycline were replaced every 2 days. Tumors were measured 3 times per week and the volumes were calculated using the formula V=(length x width^2)/2. Doxycycline was acquired from Sigma (D9891-10G). To evaluate *in vivo* effects of GSK126 the AGR129 mice were subcutaneously injected with 3 x 10^6 Karpas422 cells in 200μl volume of 1:1 PBS:Matrigel. When palpable tumors were established, vehicle (20% SBE-β-CD adjusted to pH 4-4.5 with 1N acetic acid) or GSK126 at concentration of 150 mg/kg were daily injected (during 10 days) in the final volume of 0.2ml per injection as previously described [35].

Statistical Analysis

All data are representative of at least three different experiments. Statistical significance was ascertained by performing appropriate tests described in figure legends. Significant differences were indicated by * (p≤0.05), ** (p≤0.01) or *** (p≤0.001).

Data-mining from published microarray data sets

Raw expression profiles (CEL files) were downloaded from the publicly available data-sets (GSE10846 [36], GSE23501 [37], GSE40971[35], GSE56315 [38]) imported and normalized using RMA (Robust Multiarray Average) algorithm in Partek Genomics Suite 6.4 (Partek, St. Louis, MO,

6

USA). Differences of expression between groups using the Wilcoxon rank-sum test and Pearson correlations were calculated using Stata/SE v.12.1 (StataCorp, College Station, TX, USA), the Pearson correlations P values with the tool available at www.socscistatistics.com. Genes were considered differentially expressed between groups if bearing a p<0.005, q-value <0.05 and an absolute log ratio > 0.3 in both cohorts.

Results

IRE1 signaling is defective in a subset of diffuse large B cell lymphomas

In conditions of ER stress IRE1 engages its endoribonuclease activity to promote unconventional processing of *XBP1* mRNA leading to production of mature, spliced *XBP1* mRNA. The spliced *XBP1* mRNA product is consequently translated into the active transcription factor XBP1s. Gene expression profiles have indicated that ABC DLBCLs express XBP1 target genes at higher levels than GCB DLBCLs. This suggested that the IRE1/XBP1 pathway is differentially regulated between the two DLBCL subtypes and led to the hypothesis that ABC DLBCL display enhanced basal XBP1s protein [34]. To further evaluate this, we studied IRE1 activity in four representative DLBCL cell lines. To trigger IRE1 activation, we treated DLBCL cells with tunicamycin, an inhibitor of N-linked glycosylation that triggers robust ER-stress, and measured gene expression. The induction of XBP1 target genes was impaired in the representative GCB DLBCL lines compared to ABC DLBCL cells (Figure 1A). Along these lines, XBP1 mRNA maturation and XBP1s protein expression were almost completely abolished in these two GCB DLBCL lines (Figure 1B). Inability of GCB DLCBL cells to splice XBP1 mRNA was combined with reduced levels of IRE1 protein (Figure 1B), indicating that IRE1 downregulation may impair the activation of a functional ER-stress response in GCB DLBCL cells. To extend these findings further, we analyzed a larger panel of DLBCL cell lines and found that 9 out of 11 GCB DLBCL

cells had an impaired IRE1 expression that correlated with defective production of active XBP1s upon 6 hours treatment with tunicamycin (Figure 1C). In line with these observations, we found that ER-stress mediated induction of the XBP1 target gene *DNAJB9* was impaired in GCB DLBCL compared to ABC DLBCL (Supplemental Figure 1A) while expression of the RIDD target *Bloc1S1* mRNA, was not affected upon ER-stress induction in GCB DLBCL (Supplemental Figure 1B), further indicating that IRE1 functions are defective in GCB DLBCL. Importantly, other ER stress response pathways were similar in both subtypes, as measured by ATF6 and PERK levels (Figure 1C). Moreover, upon exposure to tunicamycin, PERK activation and production of its downstream effectors, phospho-eIF2α and ATF4, were unaffected in GCB DLBCL cells (Figure 1C and Supplemental Figure 1C and 1D). This indicated that these cells can mount a response to tunicamycin and do not display a global ER-stress response defect but rather a specific down-modulation of the IRE1/XBP1 signaling branch. Next, we treated DLBCL with various pharmacological inducers of ER-stress pathways. Administration of proteasome inhibitor bortezomib led to specific activation of PERK-ATF4 pathway without promoting robust IRE1-XBP1 activation in both subtypes. However, treatment with other stress inducers such as thapsigargin, dithiothreitol (DTT), brefeldin A or nelfinavir specifically affected production of XBP1s in representative GCB cells when compared to ABC DLBCL (Figure 1D, Supplemental Figure 1E). In stark contrast, IRE1 levels and response appeared functional in other experimental models, such as Jurkat T cell leukemia cells, lymphoblastoid B-cell line CB33, human blood B cells and in panel of Burkitt's lymphomas that similar to GCB DLBCL are germinal center B-cell-derived cancers (Supplemental Figure 2A-D).

To interrogate whether IRE1 expression modulated the ability of DLBCL to cope with stress, we monitored cell viability in a panel of IRE1 high and IRE1 low DLBCL treated with the stress inducers tunicamycin or nelfinavir. Cells with reduced IRE1 displayed a significantly impaired

viability in presence of stress (Figure 1E), indicating that decreased IRE1 expression affected optimal stress-adaption programs in GCB DLBCL.

IRE1 expression is regulated at transcriptional level in GCB DLBCL

The identification of cell types that downregulate IRE1 to non-functional levels, revealed an unanticipated mechanism of regulation of the ER-stress response. IRE1 is expected to be expressed and functional in virtually all eukaryotic cells to elicit a swift response to homeostatic changes. To investigate protein degradation mechanisms that may regulate its expression, we monitored IRE1 protein levels in presence of the proteasome inhibitor MG132. As expected we found that proteasome inhibition stabilized XBP1 unspliced (XBP1u) protein [39] in GCB DLCBL cells similar to the protein levels observed in ABC DLBCL (Figure 2A). This indicated that GCB DLBCL cells are capable of producing *XBP1* mRNA. However no recovery of IRE1 protein expression or XBP1s production was observed in GCB DLBCL cells (Figure 2A). This suggests that proteasomal degradation of IRE1 does not contribute to the observed IRE1 phenotype in this lymphoma subtype. To investigate whether IRE1 regulation occurred at the transcriptional level, we analyzed *IRE1* mRNA expression in a dataset profiling GCB DLBCL tumors and tonsil-derived B cell subtypes [38] and observed that *IRE1* expression was reduced in GCB DLBCL compared to normal B cells, including germinal center B cells (Supplemental Figure 2E). Then, we investigated *IRE1* mRNA expression in two genes expression datasets profiling 167 ABC and 183 GCB DLBCL tumors [36]. In both groups, clinical samples classified as GCB DLBCL had significantly lower *IRE1* mRNA expression compared to ABC DLBCL tumors (Figure 2B). Similarly, *IRE1* mRNA levels in DLBCL cell lines were significantly reduced in GCB DLBCL cells compared to ABC DLBCL cells (Figure 2C). In contrast, other stress related genes, such as *ATF4*, *Chop*, *PERK* and *ATF6* were not significantly reduced in GCB DLBCL compared to ABC

DLBCL (Figure 2D and E; Supplemental Figure 3). Thus, *IRE1* mRNA downregulation is a hallmark of GCB DLBCL tumors that occurs independently of the other branches of the ER-stress response.

EZH2 regulates IRE1 expression in DLBCL

Gain-of-function EZH2 mutations are typical features that discriminate GCB from ABC DLBCL [17,40]. EZH2 is the catalytic subunit of the PRC2 complex that catalyzes the mono through trimethylation of lysine 27 on histone H3 (H3K27). Trimethylation of H3K27 suppresses transcription of specific genes that are proximal to the site of histone modification, a mechanism that may contribute to tumor growth [41]. Previously it has been demonstrated that in GCB DLBCL, through the generation of *de novo* bivalent domains, EZH2 downregulates the genes involved in plasma cell differentiation and keeps the tumors arrested in germinal center-like developmental stage [23]. In the two available DLBCL genes expression-profiling datasets [36], we observed that within the GCB DLBCL clinical samples *EZH2* expression negatively correlated with *IRE1* mRNA levels (Figure 3A). No such correlation was observed between *EZH2* and *PERK* expression levels (Supplemental Figure 4A). Moreover, analysis of gene expression profile datasets from GCB patients [37] and GCB cell lines [35] indicated that EZH2 gain-of-function mutations correlated with decreased IRE1 expression (Figure 3B and Supplemental Figure 4B). To confirm that EZH2 modulates IRE1 expression and stress responses, we generated HeLa cells expressing EZH2 gain-of-function mutant form (Y641F) that is typically observed in GCB DLBCL [18]. Compared to control cells, EZH2^{Y641F}-expressing cells showed increased levels of H3K27me3 while IRE1 expression was reduced (Supplemental Figure 4C). Consistently, IRE1-mediated gene expression upon treatment with tunicamycin was impaired in EZH2^{Y641F}-expressing cells (Supplemental figure 4D). This suggested that EZH2 could specifically silence

IRE1 expression through epigenetic modification of its promoter. To test this hypothesis we measured by chromatin immunoprecipitation (ChIP) H3K27me3 marks within the proximal promoter region of IRE1 and found that GCB cells displayed an increased enrichment of H3K27me3 marks compared to ABC cells (Figure 3C). As expected IRF4, an EZH2 regulated gene in GCB [19] showed a similar profile. In contrast, the promoters of the house-keeping gene GAPDH and of the constitutively expressed Bcl6 gene had no detectable H3K27me3 marks while the differentiation factors MyoD and HoxA7 harbored H3K27me3 marks in both ABC and GCB cells as previously reported [23]. In addition to repressive marks, we noticed that the IRE1 promoter harbored H3K4me3 activating marks (Supplemental Figure 4E), suggesting that its activity is poised and could potentially be restored by erasing the H3K27me3 marks [42]. To test this we treated cells with a cell permeable EZH2 inhibitor GSK343 [43]. EZH2 inhibition decreased H3K27me3 marks on the IRE1 promoter (Figure 4A) and increased *IRE1* mRNA (Supplemental Figure 4F) and protein levels in the GCB subtypes (Figure 4C). Increased IRE1 expression correlated with decreased overall H3K27 trimethylation in GCB cells. In contrast PERK expression was not significantly affected by EZH2 inhibition, further demonstrating that the two ER-stress signaling branches are controlled by different mechanisms. Finally, EZH2 inhibition restored IRE1 functionality in GCB cells as demonstrated by the production of active XBP1s in presence of tunicamycin (Figure 4C). To rule out the possibility that the effects on IRE1 expression are exclusive to GSK343 we treated the cells with GSK126, another selective EZH2 inhibitor [35]. We demonstrated that, similar to GSK343, GSK126 increased IRE1 levels in various GCB DLBCL lines (Supplemental Figure 4G). Then we analyzed whether this effect could be reproduced *in vivo*. We implanted Karpas422 GCB DLBCL into immunodeficient AGR129 (IFN-α/β, IFN-γ receptor and RAG-2 deficient) mice [44] and treated the animals with GSK126 for ten days. Analysis of postmortem tumor biopsies showed that pharmacological EZH2 inhibition

in vivo promoted IRE1 protein and mRNA expression and increased the levels of the XBP1 target gene *DNAJB9* (Figure 4D and 4E). Altogether these data show that increased EZH2 activity in DLBCL contributes to decreased IRE1 levels and that pharmacological inhibition of H3K27 trimethylation can restore a functional IRE1 pathway.

Enhanced EZH2 activity regulates IRE1 levels in different tumor types

EZH2 function is predominant during embryonic development and in differentiating tissues, however its activity decreases in the majority of differentiated cells [45]. Nevertheless, aberrantly increased EZH2 activity has been reported in multiple malignancies including cervical cancer [41] [46,47]. To assess the epigenetic status of *IRE1* promoter in the context of another malignancy characterized by increased EZH2 activity, we quantified *IRE1* histone modifications in cervical cancer-derived HeLa cells (Supplemental Figure 5A). We observed that repressive (H3K27me3) and activating (H3K4me3) marks coexisted at the IRE1 promoter, indicating promoter bivalency in this cancer cell line. In contrast to GCB DLBCL and HeLa cells, *IRE1* promoter from non-tumoral mouse embryonic fibroblasts was labeled only with the activating H3K4me3 epigenetic mark (Supplemental Figure 5B). Next, we tested whether EZH2 inhibition affected IRE1 expression in HeLa cells. These cells have detectable IRE1 levels, yet in presence of EZH2 inhibitor, we observed an increase in IRE1 protein that correlated with a decrease in H3K27 trimethylation (Supplemental Figure 5C). Similarly, *IRE1* mRNA was augmented upon EZH2 inhibition (Supplemental Figure 5D). Consistently, upon deletion of the *EZH2* gene by CRISR/Cas9, IRE1 expression was increased, enhancing XBP1s protein production in presence of mild ER-stress (Supplemental Figure 5E). These data indicate that in different tumors characterized by enhanced EZH2 function, IRE1 expression levels are predefined by aberrant epigenetic activity that controls its signaling outputs.

Reactivation of the IRE1 pathway contributes to toxic effects of EZH2 inhibitors in GCB DLBCL

EZH2 inhibition was demonstrated to be specifically toxic to GCB lymphomas [23,35]. Similar to previous reports we observed that EZH2 inhibition with GSK343 predominantly affected GCB growth *in vitro* (Supplemental Figure 6A). To evaluate the contribution of IRE1, we generated IRE1 deficient SUDHL4 (GCB DLBCL) cells (Figure 4F) and analyzed cell viability upon treatment with GSK343. We found that EZH2 inhibition mediated toxicity was reduced in IRE1 deficient clones compared to controls (Figure 4G). These data indicate that reactivation of the IRE1 pathway contributes, at least partially, to the anti-tumoral effects of EZH2 inhibitors.

Expression of XBP1s impairs tumor growth in a GCB DLBCL xenograft model

Because aberrantly decreased IRE1-XBP1s pathway is a feature of most GCB DLBCL, we interrogated the contribution of this pathway to tumor growth. We generated HBL1 (ABC DLBCL) and SUDHL4 (GCB DLBCL) cells that produce a doxycycline-inducible XBP1s protein. These cells were transplanted into the flanks of immunodeficient AGR129 mice [44], and tumor growth was monitored over time. We found that doxycycline administration did not affect growth of the ABC tumors (Figure 5A). On the other hand, treatment with doxycycline resulted in impaired growth of the grafted GCB tumors (Figure 5C). As expected, analysis of post-mortem tumor biopsies showed that, in both models, doxycycline administration increased XBP1s expression and its downstream target *DNAJB9* (Figure 5B and 5D). Interestingly, in the GCB xenograft model XBP1s induced expression of the pro-apoptotic gene *Chop* (Figure 5D). Doxycycline *per se*, did not impair the growth of tumors originating from parental HBL1 and SUDHL4 cells (Supplemental Figure 7A and 7C). Similarly, this treatment did not promote the transcription of *DNAJB9* as measured in the tumor biopsies (Supplemental Figure 7B and 7D).

These data indicate that XBP1s can decrease tumor growth in GCB DLBCL, further suggesting that decreased IRE1 activation in particular cancers types may contribute to tumorigenesis [48].

Discussion

Here, we demonstrate that EZH2 mediated epigenetic regulation pre-defines basal IRE1 expression levels. In GCB DLBCL, where EZH2 frequently carries gain-of-function mutations, *IRE1* promoter is labeled by high amounts of H3K27me3 repressive marks. This promotes IRE1 down-regulation and blunts ER stress responses as demonstrated by inability of GCB DLBCL to activate XBP1 or downregulate the targets of IRE1-mediated mRNA decay. IRE1 expression and function could be restored upon EZH2 inhibition, demonstrating the role of this regulation in DLBCL. Additionally, in a cervical cancer cell line, characterized by enhanced EZH2 activity, we observed a similar mode of epigenetic downregulation of the *IRE1* promoter, indicating that this regulatory mechanism is conserved among different tumors.

The IRE1-XBP1 pathway plays an important role in secretory cell differentiation and maintenance [30,49]. It is therefore conceivable that differentiation programs may engage epigenetic modifiers to establish IRE1 protein levels and therefore couple ER-stress response capacity to the physiological requirements. In line with this hypothesis EZH2 has been involved in the differentiation and maintenance of secretory cells including pancreatic β-cells [50]. Similarly, EZH2 regulates the genetic programs associated with differentiation of germinal center B-cells to plasma cells or memory B-cells [19,23], a process that is also dependent on the IRE1-XBP1 pathway [24,26]. The mechanisms involved in IRE1 activation during B cell differentiation are still poorly understood. Studies have shown that XBP1s production in this context precedes ER-stress [51]. Our findings indicating that EZH2 status regulates IRE1 expression raise the question of whether, during B cells differentiation, increased IRE1 expression could be mediated by decreased EZH2

14

activity [52]. It was shown that overexpression of IRE1 promotes its own activation [53], thus enhanced IRE1 expression during differentiation could be sufficient to initiate the pathway and trigger XBP1s production.

In multiple myeloma, activation of the IRE1-XBP1s signaling pathway has been considered as a tumor-promoting event [31,33,54]. In contrast, here we found that in GCB DLBCL this pathway affects tumor growth and is therefore downregulated . Reconstitution of XBP1s signaling specifically impaired the growth of GCB DLBCL tumors *in vivo*. These data highlight the key role of the IRE1-XBP1 pathway in malignancies and suggest that it can contribute to both, tumor-promoting and tumor-repressing roles depending on the tumor type.

While our results indicate that XBP1s is an important regulator of GCB DLBCL growth downstream of IRE1, we cannot exclude that other pathways steaming from IRE1, such as RIDD, could also play a role and further affect GCB tumor growth. XBP1 may regulate GCB DLBCL tumors by different mechanisms. It drives expression of the UPR network genes that is a hallmark of plasma cell differentiation [30]. Therefore, decreasing XBP1s production, by means of EZH2-mediated inhibition of IRE1 may contribute to differentiation arrest and thereby promote tumorigenesis in GCB DLBCL. In addition we observed that expression of the pro-apoptotic gene *Chop* was induced downstream XBP1s exclusively in GCB DLBCL. It is therefore possible that XBP1s directly engages pro-apoptotic programs that may contribute to decreased tumor growth in this lymphoma subtype.

The identification of mechanisms controlling IRE1 expression in DLBCL suggests that differences in the XBP1 signatures between ABC and GCB DLBCL [34] could be a consequence of the specific down-regulation of IRE1 signaling observed in GCB DLBCL. Despite a possible scenario where, due to an advanced differentiation state, IRE1 activation takes place in some

ABC tumors, we clearly demonstrated that GCB cells suffer an obvious shortage in IRE1 expression and downstream XBP1 signaling. Therefore we suggest that IRE1 expression level could be a robust biomarker of DLBCL classification.

While we cannot exclude that additional mechanisms may contribute to IRE1 downregulation in GCB DLBCL, the fact that the pathway could be restored *in vivo* upon treatment with EZH2 inhibitors is quite remarkable. This indicates that these drugs that have been developed as cancer therapeutics [41] could be positioned to modulate ER-stress responses in human diseases characterized by epigenetic deregulation of the IRE1/XBP1 pathway [55]. Because IRE1 plays a role in tumorigenesis [33,54,56], it would be important to interrogate how these drugs affect ER-stress responses and what consequences this may have on tumor progression in treated patients.

IRE1 is a key pathway that determines cellular fate in various tissues and cancers. Emerging regulatory mechanisms that tune IRE1 expression and function, such as EZH2, could play an important role in various pathologies and conditions. It is therefore likely that further studies of these mechanisms will uncover their importance beyond their role in DLBCL, including during differentiation programs, in the course of stress responses and in other tumors.

research grant of the Gelu Foundation. BB is supported by a fellowship of the ISREC foundation.

Author Contributions

Conceptualization, F.M and B.B.; Methodology, B.B. and F.M.; Investigation, B.B. A.D.G, R.T., S.C., F,B., O.D. and L.Z.; Writing - Original Draft, F.M. and B.B.; Funding Acquisition, F.M. B.B.; Resources, F.B., M.G.; Supervision, F.M.

Conflict of Interest

The authors declare no competing interests

References

1.   Lenz G, Staudt LM. Aggressive lymphomas. *N Engl J Med*. 2010;362(15):1417-1429.
2.   Alizadeh AA, Eisen MB, Davis RE, et al. Distinct types of diffuse large B-cell lymphoma identified by gene expression profiling. *Nature*. 2000;403(6769):503-511.
3.   Lenz G, Wright GW, Emre NC, et al. Molecular subtypes of diffuse large B-cell lymphoma arise by distinct genetic pathways. *Proc Natl Acad Sci U S A*. 2008;105(36):13520-13525.
4.   Roschewski M, Staudt LM, Wilson WH. Diffuse large B-cell lymphoma-treatment approaches in the molecular era. *Nat Rev Clin Oncol*. 2014;11(1):12-23.
5.   Ngo VN, Davis RE, Lamy L, et al. A loss-of-function RNA interference screen for molecular targets in cancer. *Nature*. 2006;441(7089):106-110.
6.   Lenz G, Davis RE, Ngo VN, et al. Oncogenic CARD11 mutations in human diffuse large B cell lymphoma. *Science*. 2008;319(5870):1676-1679.
7.   Davis RE, Ngo VN, Lenz G, et al. Chronic active B-cell-receptor signalling in diffuse large B-cell lymphoma. *Nature*. 2010;463(7277):88-92.
8.   Ngo VN, Young RM, Schmitz R, et al. Oncogenically active MYD88 mutations in human lymphoma. *Nature*. 2011;470(7332):115-119.
9.   Hailfinger S, Lenz G, Ngo V, et al. Essential role of MALT1 protease activity in activated B cell-like diffuse large B-cell lymphoma. *Proc Natl Acad Sci U S A*. 2009;106(47):19946-19951.
10.   Pasqualucci L, Compagno M, Houldsworth J, et al. Inactivation of the PRDM1/BLIMP1 gene in diffuse large B cell lymphoma. *J Exp Med*. 2006;203(2):311-317.
11.   Calado DP, Zhang B, Srinivasan L, et al. Constitutive canonical NF-kappaB activation cooperates with disruption of BLIMP1 in the pathogenesis of activated B cell-like diffuse large cell lymphoma. *Cancer Cell*. 2010;18(6):580-589.
12.   Ye BH, Lista F, Lo Coco F, et al. Alterations of a zinc finger-encoding gene, BCL-6, in diffuse large-cell lymphoma. *Science*. 1993;262(5134):747-750.
13.   Klein U, Dalla-Favera R. Germinal centres: role in B-cell physiology and malignancy. *Nat Rev Immunol*. 2008;8(1):22-33.

14.   Shaffer AL, Yu X, He Y, Boldrick J, Chan EP, Staudt LM. BCL-6 represses genes that function in lymphocyte differentiation, inflammation, and cell cycle control. *Immunity*. 2000;13(2):199-212.

15.   Cattoretti G, Pasqualucci L, Ballon G, et al. Deregulated BCL6 expression recapitulates the pathogenesis of human diffuse large B cell lymphomas in mice. *Cancer Cell*. 2005;7(5):445-455.

16.   Cerchietti LC, Ghetu AF, Zhu X, et al. A small-molecule inhibitor of BCL6 kills DLBCL cells in vitro and in vivo. *Cancer Cell*. 2010;17(4):400-411.

17.   Morin RD, Johnson NA, Severson TM, et al. Somatic mutations altering EZH2 (Tyr641) in follicular and diffuse large B-cell lymphomas of germinal-center origin. *Nat Genet*. 2010;42(2):181-185.

18.   Yap DB, Chu J, Berg T, et al. Somatic mutations at EZH2 Y641 act dominantly through a mechanism of selectively altered PRC2 catalytic activity, to increase H3K27 trimethylation. *Blood*. 2011;117(8):2451-2459.

19.   Caganova M, Carrisi C, Varano G, et al. Germinal center dysregulation by histone methyltransferase EZH2 promotes lymphomagenesis. *J Clin Invest*. 2013;123(12):5009-5022.

20.   Beguelin W, Teater M, Gearhart MD, et al. EZH2 and BCL6 Cooperate to Assemble CBX8-BCOR Complex to Repress Bivalent Promoters, Mediate Germinal Center Formation and Lymphomagenesis. *Cancer Cell*. 2016;30(2):197-213.

21.   Cedar H, Bergman Y. Linking DNA methylation and histone modification: patterns and paradigms. *Nat Rev Genet*. 2009;10(5):295-304.

22.   Voigt P, Tee WW, Reinberg D. A double take on bivalent promoters. *Genes Dev*. 2013;27(12):1318-1338.

23.   Beguelin W, Popovic R, Teater M, et al. EZH2 is required for germinal center formation and somatic EZH2 mutations promote lymphoid transformation. *Cancer Cell*. 2013;23(5):677-692.

24.   Iwakoshi NN, Lee AH, Vallabhajosyula P, Otipoby KL, Rajewsky K, Glimcher LH. Plasma cell differentiation and the unfolded protein response intersect at the transcription factor XBP-1. *Nat Immunol*. 2003;4(4):321-329.

25.   Iwawaki T, Akai R, Kohno K. IRE1alpha disruption causes histological abnormality of exocrine tissues, increase of blood glucose level, and decrease of serum immunoglobulin level. *PLoS One*. 2010;5(9):e13052.

26.   Reimold AM, Iwakoshi NN, Manis J, et al. Plasma cell differentiation requires the transcription factor XBP-1. *Nature*. 2001;412(6844):300-307.

27.   Hollien J, Lin JH, Li H, Stevens N, Walter P, Weissman JS. Regulated Ire1-dependent decay of messenger RNAs in mammalian cells. *J Cell Biol*. 2009;186(3):323-331.

28.   Hetz C, Martinon F, Rodriguez D, Glimcher LH. The unfolded protein response: integrating stress signals through the stress sensor IRE1alpha. *Physiol Rev*. 2011;91(4):1219-1243.

29.   Lee AH, Iwakoshi NN, Glimcher LH. XBP-1 regulates a subset of endoplasmic reticulum resident chaperone genes in the unfolded protein response. *Mol Cell Biol*. 2003;23(21):7448-7459.

30.   Shaffer AL, Shapiro-Shelef M, Iwakoshi NN, et al. XBP1, downstream of Blimp-1, expands the secretory apparatus and other organelles, and increases protein synthesis in plasma cell differentiation. *Immunity*. 2004;21(1):81-93.

31.   Carrasco DR, Sukhdeo K, Protopopova M, et al. The differentiation and stress response factor XBP-1 drives multiple myeloma pathogenesis. *Cancer Cell*. 2007;11(4):349-360.

32.   Mimura N, Fulciniti M, Gorgun G, et al. Blockade of XBP1 splicing by inhibition of IRE1alpha is a promising therapeutic option in multiple myeloma. *Blood*. 2012;119(24):5772-5781.

33.   Papandreou I, Denko NC, Olson M, et al. Identification of an Ire1alpha endonuclease specific inhibitor with cytotoxic activity against human multiple myeloma. *Blood*. 2011;117(4):1311-1314.

34.   Shaffer AL, Wright G, Yang L, et al. A library of gene expression signatures to illuminate normal and pathological lymphoid biology. *Immunol Rev*. 2006;210:67-85.

35.   McCabe MT, Ott HM, Ganji G, et al. EZH2 inhibition as a therapeutic strategy for lymphoma with EZH2-activating mutations. *Nature*. 2012;492(7427):108-112.

36.   Lenz G, Wright G, Dave SS, et al. Stromal gene signatures in large-B-cell lymphomas. *N Engl J Med*. 2008;359(22):2313-2323.

37.   Shaknovich R, Geng H, Johnson NA, et al. DNA methylation signatures define molecular subtypes of diffuse large B-cell lymphoma. *Blood*. 2010;116(20):e81-89.

38.   Dybkaer K, Bogsted M, Falgreen S, et al. Diffuse large B-cell lymphoma classification system that associates normal B-cell subset phenotypes with prognosis. *J Clin Oncol*. 2015;33(12):1379-1388.

39.   Tirosh B, Iwakoshi NN, Glimcher LH, Ploegh HL. Rapid turnover of unspliced Xbp-1 as a factor that modulates the unfolded protein response. *J Biol Chem*. 2006;281(9):5852-5860.

40.   Sneeringer CJ, Scott MP, Kuntz KW, et al. Coordinated activities of wild-type plus mutant EZH2 drive tumor-associated hypertrimethylation of lysine 27 on histone H3 (H3K27) in human B-cell lymphomas. *Proc Natl Acad Sci U S A*. 2010;107(49):20980-20985.

41.   Kim KH, Roberts CW. Targeting EZH2 in cancer. *Nat Med*. 2016;22(2):128-134.

42.   Bernstein BE, Mikkelsen TS, Xie X, et al. A bivalent chromatin structure marks key developmental genes in embryonic stem cells. *Cell*. 2006;125(2):315-326.

43.   Verma SK, Tian X, LaFrance LV, et al. Identification of Potent, Selective, Cell-Active Inhibitors of the Histone Lysine Methyltransferase EZH2. *ACS Med Chem Lett*. 2012;3(12):1091-1096.

44.   Grob P, Schijns VE, van den Broek MF, Cox SP, Ackermann M, Suter M. Role of the individual interferon systems and specific immunity in mice in controlling systemic dissemination of attenuated pseudorabies virus infection. *J Virol*. 1999;73(6):4748-4754.

45.   Herviou L, Cavalli G, Cartron G, Klein B, Moreaux J. EZH2 in normal hematopoiesis and hematological malignancies. *Oncotarget*. 2016;7(3):2284-2296.

46.   Ding M, Zhang H, Li Z, et al. The polycomb group protein enhancer of zeste 2 is a novel therapeutic target for cervical cancer. *Clin Exp Pharmacol Physiol*. 2015;42(5):458-464.

47.   Cai L, Wang Z, Liu D. Interference with endogenous EZH2 reverses the chemotherapy drug resistance in cervical cancer cells partly by up-regulating Dicer expression. *Tumour Biol*. 2016;37(5):6359-6369.

48.   Chevet E, Hetz C, Samali A. Endoplasmic reticulum stress-activated cell reprogramming in oncogenesis. *Cancer Discov*. 2015;5(6):586-597.

49.   Lee AH, Chu GC, Iwakoshi NN, Glimcher LH. XBP-1 is required for biogenesis of cellular secretory machinery of exocrine glands. *EMBO J*. 2005;24(24):4368-4380.

50.   Chen H, Gu X, Su IH, et al. Polycomb protein Ezh2 regulates pancreatic beta-cell Ink4a/Arf expression and regeneration in diabetes mellitus. *Genes Dev*. 2009;23(8):975-985.

51.   Hu CC, Dougan SK, McGehee AM, Love JC, Ploegh HL. XBP-1 regulates signal transduction, transcription factors and bone marrow colonization in B cells. *EMBO J*. 2009;28(11):1624-1636.

52.   Velichutina I, Shaknovich R, Geng H, et al. EZH2-mediated epigenetic silencing in germinal center B cells contributes to proliferation and lymphomagenesis. *Blood*. 2010;116(24):5247-5255.

53.   Welihinda AA, Tirasophon W, Green SR, Kaufman RJ. Protein serine/threonine phosphatase Ptc2p negatively regulates the unfolded-protein response by dephosphorylating Ire1p kinase. *Mol Cell Biol*. 1998;18(4):1967-1977.

54.   Chen X, Iliopoulos D, Zhang Q, et al. XBP1 promotes triple-negative breast cancer by controlling the HIF1alpha pathway. *Nature*. 2014;508(7494):103-107.

55.   Jiang D, Niwa M, Koong AC. Targeting the IRE1alpha-XBP1 branch of the unfolded protein response in human diseases. *Semin Cancer Biol*. 2015;33:48-56.

56.   Clarke HJ, Chambers JE, Liniker E, Marciniak SJ. Endoplasmic reticulum stress in malignancy. *Cancer Cell*. 2014;25(5):563-573.
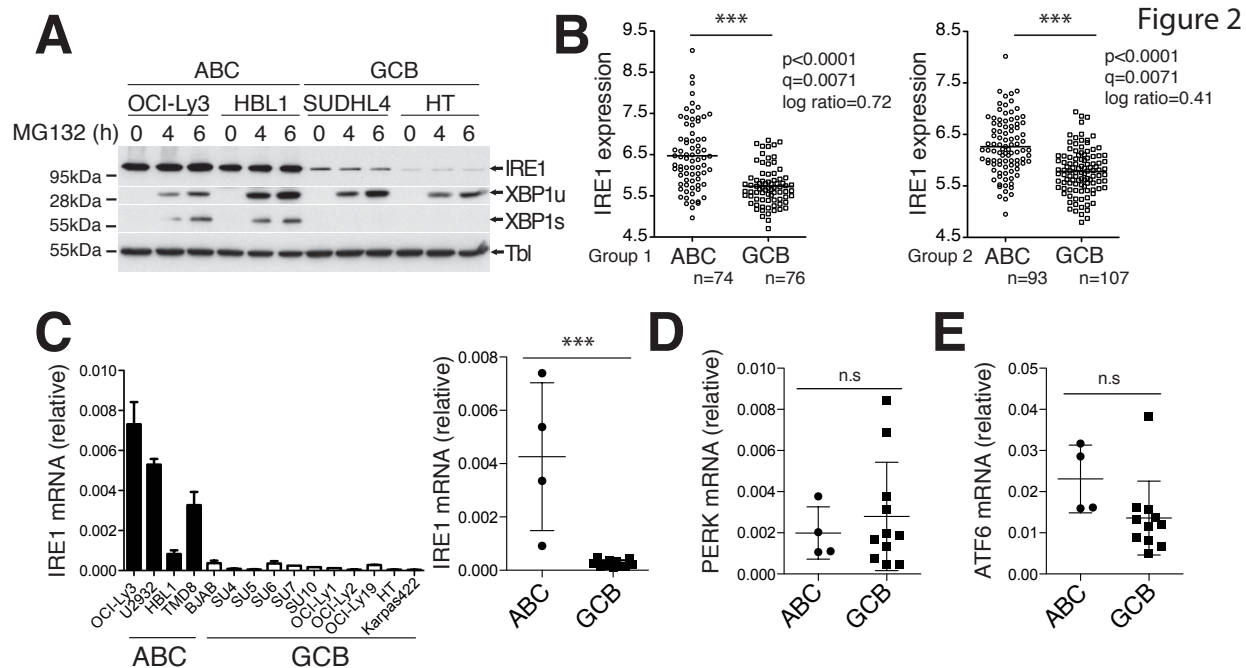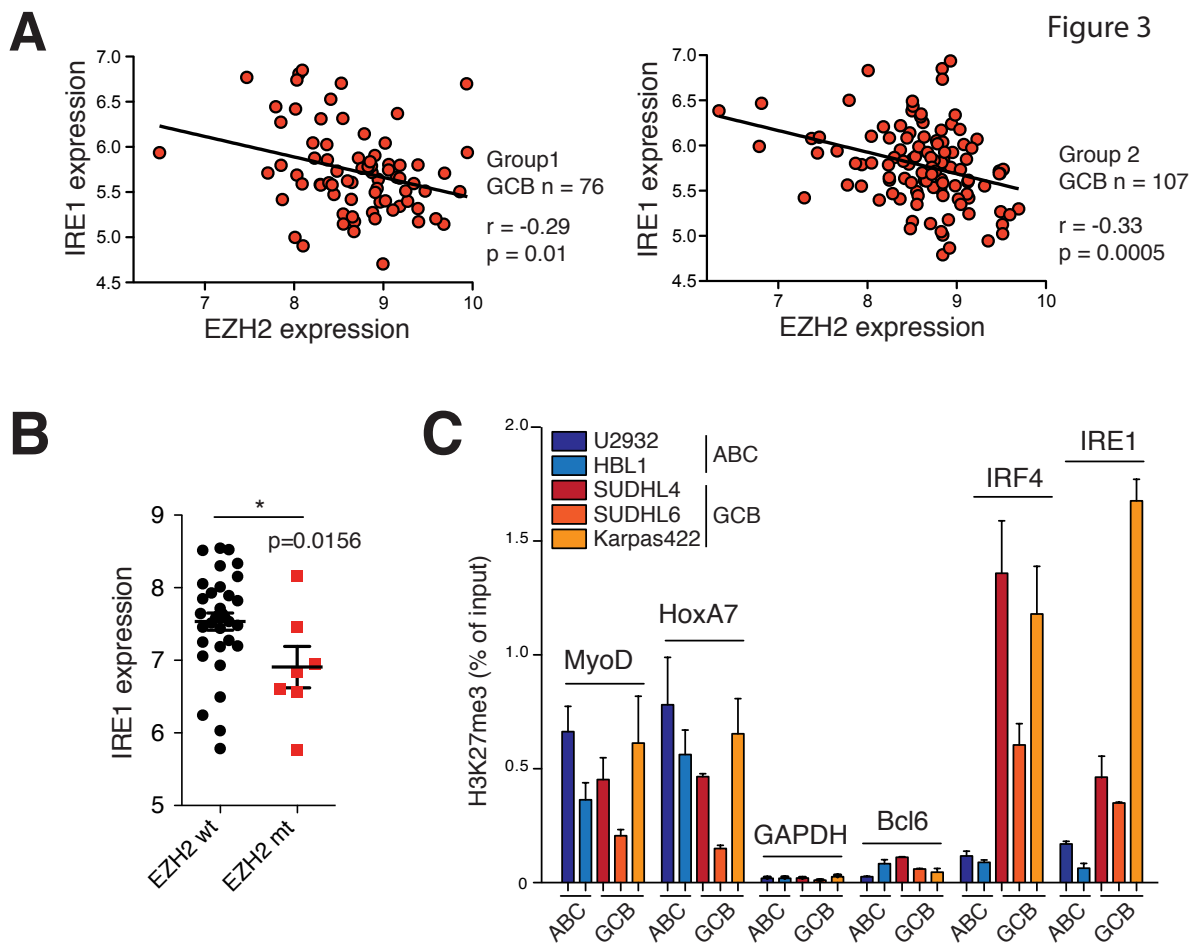
Figure:
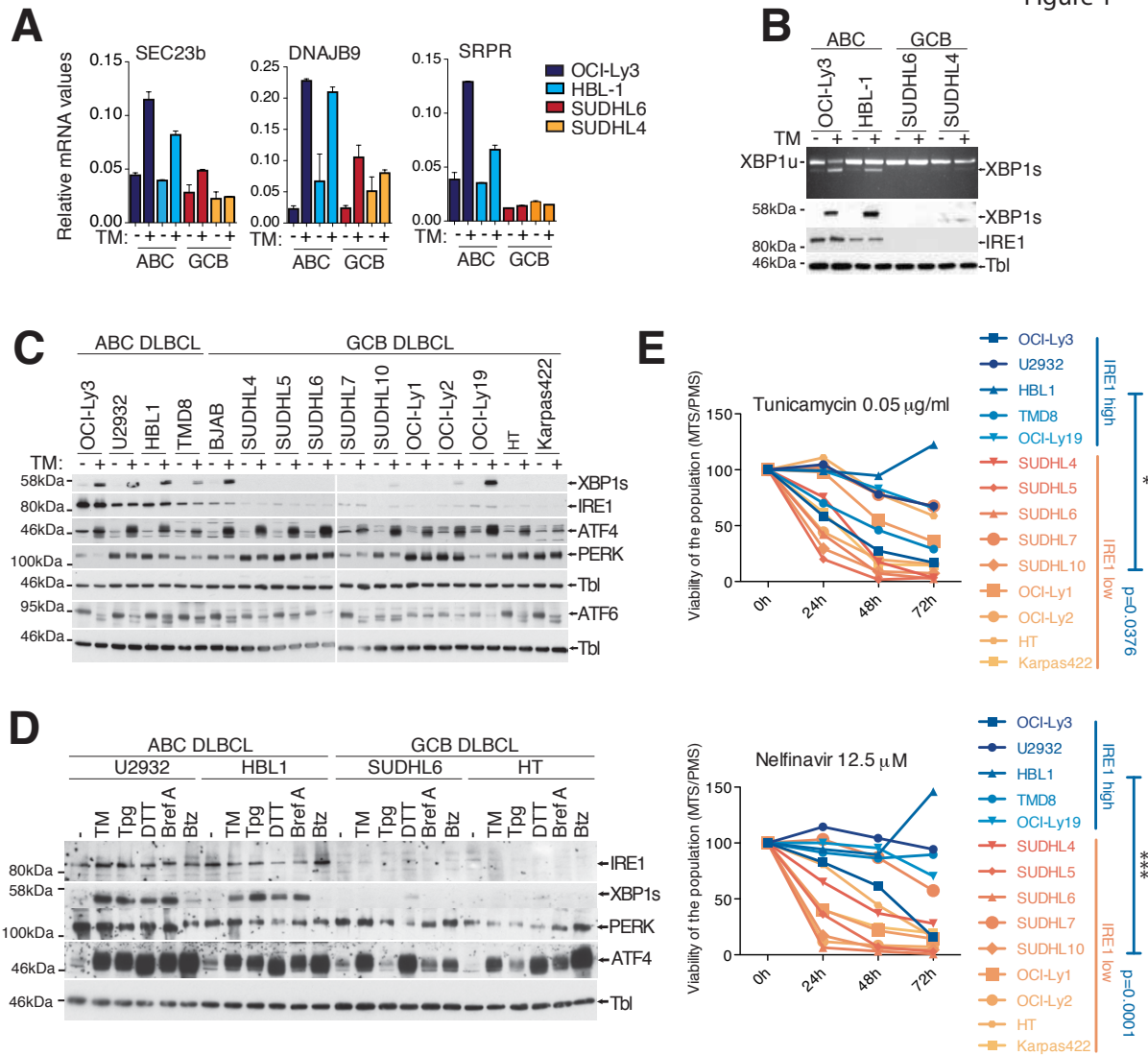
Figure 1. GCB DLBCL display impairment in IRE1 expression that affects the ER stress response. (A-B) Representative ABC DLBCL and GCB DLBCL cell lines were treated with 5 μg/ml tunicamycin (TM) for 6 h and analyzed by quantitative real-time PCR for expression of XBP1 target genes Sec23b, DNAJB9 and SRPR mRNA levels relative to β-actin (mean and SD of technical triplicates of one representative experiment out of three) (A). XBP1 mRNA splicing was measured by RT-PCR analysis of XBP1 mRNA maturation (B), DNA electrophoresis above). Protein levels of XBP1s and IRE1 protein were analyzed by immunoblot. Tubulin (Tbl) is used as loading control (B, below). (C) DLBCL cell lines were treated for 6 h with 5 μg/ml tunicamycin (TM) or vehicle and analyzed by immunoblot for XBP1s, IRE1, ATF4, PERK,

ATF6 and tubulin (Tbl). (D) Representative ABC and GCB cell lines were treated with different ER stress inducers, tunicamycin (TM), thapsigargin (Tpg), brefeldin A (Bref A), 1,4-Dithiothreitol (DTT) and Bortezomib (Btz) for 6 h. IRE1, XBP1s, PERK, ATF4 and Tubulin (Tbl) expression was analyzed by immunoblot. (E) Viability of IRE1 high and IRE1 low DLBCL cells assessed by MTS/PMS assay after treatment for the indicated time course with 0.05 µg/ml Tunicamycin or 12.5 µM Nelfinavir. P values were calculated using 2way ANOVA. * P value ≤ 0.05 *** P value ≤ 0.001

Figure 2. IRE1 mRNA levels are downregulated in GCB DLBCL. (A) 2 ABC and 2 GCB DLBCL cell lines were treated for 4 or 6 h with 10 μM proteasome inhibitor MG132. IRE1, XBP1u and XBP1s protein expression was analyzed by immunoblot. Tubulin (Tbl) is used as loading control. (B) IRE1 mRNA levels in GCB-DLBCL (GCB) compared with ABC-DLBCL (ABC) molecular subtype in two independent gene expression-profiled DLBCL datasets GSE10846. Genes were considered differentially expressed between ABC and GCB if bearing a *P* value <0.005, q-value <0.05 and an absolute log ratio > 0.3 in both cohorts. (C-E) Representative ABC and GCB DLBCL cell lines were analyzed for mRNA expression levels of IRE1 (C), PERK (D) and ATF6 (E) relative to β-actin. Relative IRE1 expression (mean and SD of technical triplicates of one representative experiment) for each cell line tested is shown in C (left panel). Statistical analyses were done using unpaired T test to compare relative mRNA expression between ABC and GCB cells. *** *P* value ≤ 0.001, ns: *P* value > 0.05.

Figure 3. IRE1 promoter in GCB DLBCL carries high levels of repressive histone mark H3K27me3. (A) Correlations as measured by the Pearson correlation coefficient r between EZH2 expression and IRE1 expression in GCB DLBCL clinical samples from two datasets extracted from GSE10846. (B) IRE1 mRNA levels in EZH2 wild type and EZH2 mutated GCB DLBCL patients. Data extracted from gene expression datasets GSE23501. Wilcoxon signed-rank test * P value ≤ 0.05 (C) Chromatin immunoprecipitation (ChIP) was performed on ABC and GCB DLBCL cell lines using H3K27me3 specific antibody. Enrichments of indicated promoters were probed by realtime PCR (mean and SD of technical triplicates of one representative experiment out of three). MyoD and Hoxa7 regions are positive controls for H3K27me3 mediated repression. GAPDH and BCL6 promoters are negative controls for H3K27me3 mediated repression.
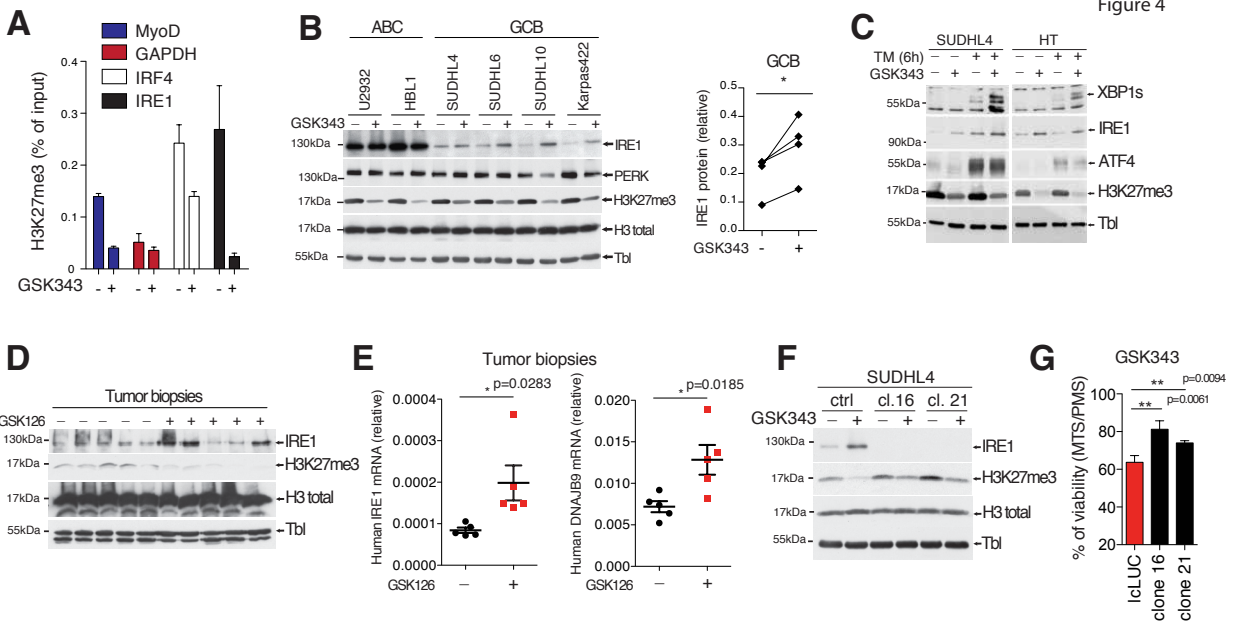
Figure 4. IRE1 expression levels and activity are regulated by histone methyltransferase EZH2. (A) Karpas422 cells treated for 5 days with 2.5 μM of the EZH2 inhibitor GSK343 or vehicle were analyzed by ChIP for H3K27me3 promoter marks on MyoD and IRF4 (EZH2 dependent), GAPDH (negative control) and IRE1 (mean and SD of technical triplicates of one representative experiment out of three). (B) Representative ABC and GCB DLBCL cell lines treated with GSK343 or vehicle were probed by immunoblot for IRE1, PERK, H3K27me3, H3 total and Tubulin (Tbl). IRE1 protein levels were quantified and plotted (right panel). Paired T test (non-treated vs. treated). * P value ≤ 0.05 (C) Representative GCB DLBCL cell lines were treated for 5 days with 2.5 μM EZH2 inhibitor GSK343. Then, 5 μg/ml tunicamycin (TM) was added to the cells for 6 h. Immunoblots were revealed using antibodies against XBP1s, IRE1, PERK, ATF4, H3K27me3 and Tubulin (Tbl). (Experiment representative of three). (D) Karpas422 cells were subcutaneously injected in immunodeficient AGR129 mice. Mice were injected during 10 days with the vehicle or 150 mg/kg GSK126 as described in Materials and Methods. IRE1, H3K27me3, H3 total and Tubulin (Tbl) levels were analyzed by immunoblot. (E) Human IRE1 and DNAJB9 relative mRNA values were assessed in postmortem biopsies. (F) Parental and IRE1 deficient SUDHL4 cells were treated for 4 days with vehicle or 5 μM GSK343. IRE1, H3K27me3, H3 total and Tubulin (Tbl) levels were assessed by immunoblot. (G) Viability of IRE1 proficient and IRE1 deficient SUDHL4 cells was assessed by MTS/PMS assay after treatment with 10 μM GSK343 for 48 h. P values were obtained using Unpaired T test. ** P value ≤ 0.01.

Figure 5
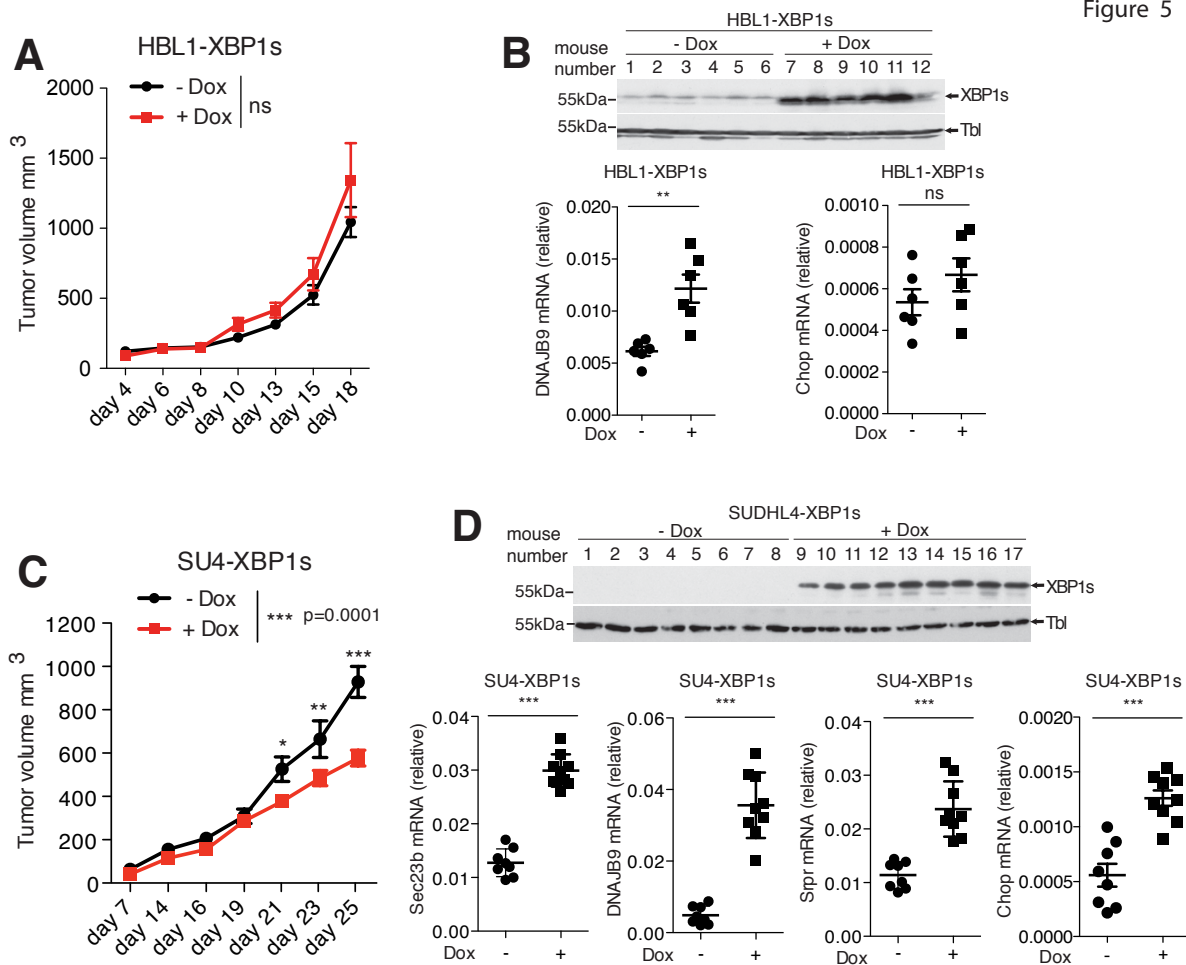
Figure 5. XBP1 signaling impairs GCB DLBCL tumor growth. (A-D) Immunodeficient AGR129 mice were injected subcutaneously with 2.5 x 10^6 HBL1 (A-B) or 3 x 10^6 SUDHL4 cells (C-D) that express XBP1s under treatment with Doxycycline. Mice were daily-administered vehicle or Doxycycline at concentration 1 mg/ml through water as described in Materials and Methods. Mean tumor volume measurements were represented against the days of treatment (A and C). *P* values were calculated using 2way ANOVA followed by Bonferroni post-test. ns: *P* value > 0.05, *P value ≤ 0.05, **P value ≤ 0.01 *** *P* value ≤ 0.001. Efficiency of Doxycycline-induced XBP1s expression and its target genes was validated by immunoblot and RQ-PCR for the mice carrying HBL1 (B) or SUDHL4 tumors (D) Each dot in the graph represents relative gene expression for a single mouse (B and D, lower panels). *P* values were calculated using Unpaired T test to compare non-treated vs. treated groups *** *P* value ≤ 0.001.